

¹Institute of Applied Chemistry, Shanxi University, Taiyuan, China

²School of Life Science, Shanxi University, Taiyuan, China

³Shanxi Academy of Analytical Sciences, Taiyuan, China

Antimicrobial compounds from *Athyrium sinense* damage the cell membrane of *Clavibacter michiganensis* subsp. *sepedonicus*

Jin Cai^{1*}, Beibei Du², Le Kang³, Junjun Guo³

(Submitted: October 31, 2019; Accepted: February 20, 2020)

Summary

Clavibacter michiganensis subsp. *sepedonicus* is a widely distributed pathogen that causes ring rot of potato. Antimicrobial activity assays demonstrated that petroleum ether extracts from *Athyrium sinense* was a fraction with strong activity against *C. michiganensis* subsp. *sepedonicus*. The aim of this study was to determine the chemical compounds in this fraction, and to investigate the antimicrobial mechanism. The dominant components were palmitic acid (25.78%), neophytadiene (13.66%), linoleic acid (8.95%), oleic acid (8.20%), phloretic acid (7.48%), methyl sinapate (6.92%), e-11-hexadecen-1-ol (6.10%), 1-hexadecanol (5.41%), and stearic acid (2.87%). Electron micrographs showed that application of the petroleum ether extracts seriously altered the morphology of *C. michiganensis* subsp. *sepedonicus*. Release of alkaline phosphatase and leakage of intracellular soluble protein confirmed that the integrity of the cell membrane was destroyed. Furthermore, ATPase activity, intracellular DNA content, and cell membrane potential were all demonstrated to be inhibited. In addition, the petroleum ether extract penetrated through the damaged cell membrane, and subsequently disrupted the cell cycle of the bacteria. We concluded that the petroleum ether fraction of ethanolic *Athyrium sinense* extracts was effective to inhibit *C. michiganensis* subsp. *sepedonicus* by damaging the cell membrane, and could be used as a natural alternative for *C. michiganensis* subsp. *sepedonicus* control.

Keywords: *Clavibacter michiganensis* subsp. *sepedonicus*; *Athyrium sinense*; bioassay-guided fraction; ring rot, antimicrobial compounds; membrane disruption

Introduction

Clavibacter michiganensis subsp. *sepedonicus* (Cms), a gram-positive bacterium, can cause bacterial ring rot of potatoes (HOLTSMARK et al., 2008). This pathogen can survive on contaminated surfaces for many years, and mainly be transmitted through seed potato during the preparation of seed cutting, or from storage facilities, organic matter, equipment and contaminated soil (CHO et al., 2015). After infecting seed potato, Cms spreads through the vascular system leading to bacterial ring rot. Symptoms of bacterial ring rot are leaf wilting and breakdown of vascular tissue. "Ring rot" means the characteristic rot of vascular tissue after the cutting of an infected tuber. Until now, bacterial ring rot has been considered a serious potato disease causing significant economic losses (NISSINEN et al., 2001). As a measure against pathogens, chemical bactericides are used for plant protection, such as copper sulfate and chlorine dioxide. However, they usually lead to environmental pollution, accumulation of toxic residues, increasing development of resistance of plant pathogens, and human health problems (ELOFF et al., 2017). Due to these serious

problems, the search for new effective strategies of inhibiting plant pathogens has become an important work (MDEE et al., 2009). For this reason, many researchers have started investigating alternatives to chemicals for controlling plant pathogens (MONSÁLVIZ et al., 2010). In order to defend against herbivores, pests, fungi, or bacteria, plants produce a lot of active compounds called secondary metabolites (MONSÁLVIZ et al., 2010). Plant-derived chemicals or plant extracts appear to play an important role in developing natural bactericides as a main substitute for chemicals, since these compounds show environmental friendliness, low toxicity, and low residue (ASANO et al., 2013).

Athyrium sinense is a species of ferns, which grows to a height of 35-60 cm with short rhizome and ovate lanceolate leaf blade (CONG and ZHANG, 2010). It is found in the forest of mountainous area in China (CONG and ZHANG, 2010). *Athyrium sinense* belongs to the family of Athyriaceae, which is one of three families of ferns (YANG et al., 2008). Several papers reported that the extracts from Athyriaceae family showed antibacterial, antifungal or antioxidant properties (ZHONG et al., 2016). In China, *A. sinense* is used in traditional medicines for treating measles, epidemic encephalitis B, epidemic cerebrospinal meningitis, influenza, and hookworm infections (CONG and ZHANG, 2010). Our previous study demonstrated that the crude ethanol extracts of *A. sinense* exhibited obvious antimicrobial activity against Cms (CAI et al., 2015). Nevertheless, the antimicrobial actions of active compounds from *A. sinense* are not understood.

Therefore, this study was to investigate the mechanisms of antimicrobial compounds from *A. sinense* against Cms. First we obtained highly active fraction from *A. sinense* ethanol extracts by bioassay-guided methods, and identified chemical compounds by gas chromatography and mass spectrometry (GC-MS). Subsequently, we observed the changes of surface morphology and internal structure by scanning electron microscope (SEM) and transmission electron microscope (TEM). Finally, we determined the integrity of plasma membrane, analyzed characterizations of intracellular materials, identified membrane potential and evaluated cell cycle.

Materials and methods

Plant material and antimicrobial compound extraction

The whole plant of *A. sinense* was collected in one batch from Pangquangou Nature Reserve (37°45′-37°55′N, 111°22′-111°33′E), Shanxi Province, China, which grew in the damp areas under the trees. *A. sinense* was washed, air-dried at room temperature under laboratory conditions and smashed by a grinder. Then, the sample was sieved by 40 mesh sieve and these powders (100 g) were extracted by 2000 mL absolute ethanol at 80±5 °C for 8 h. Ethanol extracts were concentrated by a rotary evaporator (R-1020, Henan Lanphan Technology Co., Ltd, China) at a temperature not exceeding 50 °C. The concentrated extracts were dissolved in distilled water and then were partitioned with petroleum ether, dichloromethane,

* Corresponding author

ethyl acetate, and *n*-butanol through a separating funnel (CAI et al., 2014). Partitioned extracts (petroleum ether, dichloromethane, ethyl acetate, *n*-butanol, and water fractions) were also concentrated to dryness. An aliquot of the dry residue was dissolved in 20% dimethyl sulphoxide (DMSO) to the same concentration of 10mg/mL (mg residue per ml solvent).

Antimicrobial assay

The antimicrobial activities for petroleum ether fraction, dichloromethane fraction, ethyl acetate fraction, *n*-butanol fraction, and water fraction from *A. sinense* against *Cms* were tested using the agar diffusion method. *Cms* (ATCC 33113) was the type strain and was obtained from the microbiology laboratory of Shanxi University (Taiyuan, China). *Cms* was cultivated overnight to 10^8 CFU/mL. After that, *Cms* suspension (200 μ L) was inoculated into the plate and dispersed on the surface (BEHBAHANI et al., 2017). Holes of 10 mm diameter were obtained by cutting off from agar, and then 200 μ L of each sample (10 mg residue from fractionation / mL 20% DMSO) was added into the well. Positive control was CuSO_4 (5 mg/mL). Negative control was prepared using 20% DMSO, and showed no antimicrobial activity against *Cms*. All the samples were incubated at 28 °C for 24 h. Inhibition zones around the wells were measured, and all the tests were performed in three replicates.

GC-MS analysis

The compounds of the petroleum ether fraction from *A. sinense* extract (PA; based on the result of antimicrobial assay) were analyzed by GC-MS (Trace 1310 GC and TSQ 8000 Evo triple quadrupole MS, Thermo Scientific, USA). The separation of PA was performed using a TG-5MS column (30 m length \times 0.25 mm ID \times 0.25 μ m thickness). The injection volume of PA was 1 μ L and the split ratio was 1:10. The flow of carrier gas (helium) was 1 mL/min. The warming program was set as follows: After a 3 min solvent delay, the initial temperature was 80 °C, followed by increasing to 250 °C at 4 °C min⁻¹, and holding for 3 min. The ionization voltage and ion source temperature were 70 eV and 280 °C. The mass range was from 10 amu to 650 amu. The identification of compounds from PA was carried out by comparison of the retention index (RI) and mass spectra with these stored in the database NIST 2014 (PIRAS et al., 2018). RI was determined using a series of *n*-alkanes (C7-C40, Dikma, Beijing, China). The relative percentage of each individual compound was calculated by peak area (YUAN and YUK, 2018).

SEM and TEM

The morphology observation of *Cms* was measured by scanning electron microscope (SEM) and transmission electron microscope (TEM). In brief, PA was dissolved in 0.8% DMSO, and then mixed in *Cms* cell solution (10^4 CFU mL⁻¹) for getting the concentration of 0.2 mg mL⁻¹. *Cms* cells treated with 0.80% DMSO, were used as the control. For SEM analysis (ENDO et al., 2010), samples were fixed with 2.50% (v/v) glutaraldehyde overnight and then fixed with 1% OsO_4 for 3 h, after being incubated at 28 °C for 8 h. Afterwards, *Cms* cells were dehydrated in an ascending series of ethanol (30%, 40%, 50%, 60%, 70%, 80%, 90% for 30 min, and final pure ethanol for 30 min), CO_2 critical point dried, and coated with gold-palladium (20-30 nm). Then, *Cms* cells were observed with a SEM (JSM-35C, JEOL, Japan) operating at 25 kV. For TEM analysis (XIANG et al., 2018), *Cms* pellets were obtained at 10,000 rpm for 5 min, after being incubated at 28 °C for 8 h. Samples were fixed with 2.50% (v/v) glutaraldehyde overnight and then fixed with 1% OsO_4 for 3 h. Ultrathin sections (60-90 nm) were stained with uranyl acetate and lead citrate, and were observed in a TEM (JEM-1011, JEOL, Japan) operating at 80 kV.

Measurements of cell membrane permeability and cell wall integrity

PA was dissolved in 0.80% DMSO, and then mixed in *Cms* cell solution (10^4 CFU mL⁻¹) for getting the concentration of 0.05 mg mL⁻¹, 0.10 mg mL⁻¹, 0.15 mg mL⁻¹, and 0.20 mg mL⁻¹, respectively. *Cms* cells treated with 0.8% DMSO, were used as the control. After incubation at 28 °C for 8 h, all samples (volume of each sample was 200 mL) were centrifuged at 8,000 rpm (7730 \times g) for 5 min. The alkaline phosphatase activity in supernatant was determined using the AKP assay kit (Nanjing Jiancheng Bioengineering Institute, China), and the protein contents in supernatant were measured as the soluble protein assay kit (Nanjing Jiancheng Bioengineering Institute, China). The test was performed in three replicates.

Evaluations of intracellular ATPase activity and intracellular DNA content

Cms cells were treated as described above. After incubation at 28 °C for 8 h, all samples were centrifuged at 5,000 rpm (3020 \times g) for 5 min, washed three times, and then resuspended in 0.85% sodium chloride to $\text{OD}_{600\text{nm}}=0.70$.

For ATPase activity assay, 2 ml of each sample was sonicated (2s pulse and 4s stop; 200 W) for 15 min. After centrifuging, the supernatant of each sample was determined using the ATPase activity assay kit (Nanjing Jiancheng Bioengineering Institute, China; CUI et al., 2018). The test was performed in three replicates.

For DNA content assay, 5 μ L of DAPI (0.10 mg mL⁻¹) was added into each sample (2 mL) for incubating 20 min in darkness. After removing the excess DAPI, samples were re-suspended in 2 mL of PBS. Then, 100 μ L of each sample was added into PBS (1 mL), and the fluorescence intensity of DNA in each sample was tested by a fluorescence spectrophotometer (F-280, Gangdong Sci & Tech Development Co., China; slit width of 10 nm; excitation wavelength of 364 nm; emission wavelength of 450 nm). Experiment was repeated three times.

Measurement of membrane potential

Cms cells were treated as described above (concentration of PA was 0.05 mg mL⁻¹, 0.10 mg mL⁻¹, and 0.15 mg mL⁻¹, respectively). After incubation at 28 °C for 8 h, all samples were centrifuged at 2,000 rpm (480 \times g) for 10 min, washed two times, and then resuspended in PBS. Rhodamine 123 (20 μ mol L⁻¹) was added into each sample for incubating 30min in darkness. After washing two times, each sample was tested by a FACS Calibur flow cytometer (Becton Dickinson, USA; excitation wavelength of 507 nm; emission wavelength of 529 nm).

Cell cycle analysis

Cms cells were treated as described above (concentration of PA was 0.05 mg mL⁻¹, 0.10 mg mL⁻¹, and 0.15 mg mL⁻¹, respectively). After incubation at 28 °C for 8 h, all samples were fixed with 75% alcohol in PBS overnight (4 °C), and then centrifuged and re-suspended in PI solution (50mg mL⁻¹). Each sample was tested by a FACS Calibur flow cytometer (Becton Dickinson, USA; excitation wavelength of 535 nm; emission wavelength of 615 nm).

Statistical analysis

Replicates are technical replicates, meaning repeated analysis of the same batch extract of plant material. The data were analyzed by one-way analysis of variance (ANOVA) with SPSS software (IBM, version 19.0, Armonk, USA). Duncan's multiple range test was used to analyze statistically significant differences ($P<0.05$).

Results

Determination of antimicrobial activities of five fractions from *A. sinense*

Fig. 1 showed the activity of five fractions from *A. sinense* extracts against *Cms*. As shown in Fig. 1, the inhibition zones of five fractions against *Cms* were 18.58 ± 1.46 mm (petroleum ether fraction, subsequently called PA), 14.87 ± 1.03 mm (dichloromethane fraction), 14.65 ± 0.80 mm (ethyl acetate fraction), 13.60 ± 0.60 mm (*n*-butanol fraction), and 10.20 ± 0.20 mm (water fraction), respectively. Among five fractions, petroleum ether fraction from *A. sinense* (PA) had the strongest antimicrobial activity ($P < 0.05$). Because the diameter of hole was 10 mm, 20% DMSO (inhibition zone was 10.17 ± 0.23 mm) is considered to have no antimicrobial activity against *Cms*. However, one should keep in mind that the comparison between fractions is limited since the reference base in this experiment was extract residue weight and not plant weight. Nevertheless, the PA fraction was used as the subject in the following experiments.

Chemical composition of petroleum ether fraction (PA)

As shown in Tab. 1, twenty-five components were determined by GC-MS analysis, representing 96.88% of PA. The components belonged to organic acids (59.10%), alkenes (13.66%), alcohols (12.61%), esters (9.49%), aldehydes (1.15%), and alkanes (0.87%). Palmitic acid was the major compound (25.78%), followed by neophytadiene (13.66%), linoleic acid (8.95%), oleic acid (8.20%), phloretic acid (7.48%), methyl sinapate (6.92%), *e*-11-hexadecen-1-ol (6.10%), 1-hexadecanol (5.41%), stearic acid (2.87%), 3-methylvaleric acid (2.21%), 2-hydroxy-5-methylbenzaldehyde (1.15%), 3,7,11,15-tetramethyl-2-hexadecen-1-ol (1.10%), nonanoic acid (1.04%), phenylacetic acid (1.01%), palmitic acid ethyl ester (0.93%), pentacosane (0.87%), myristic

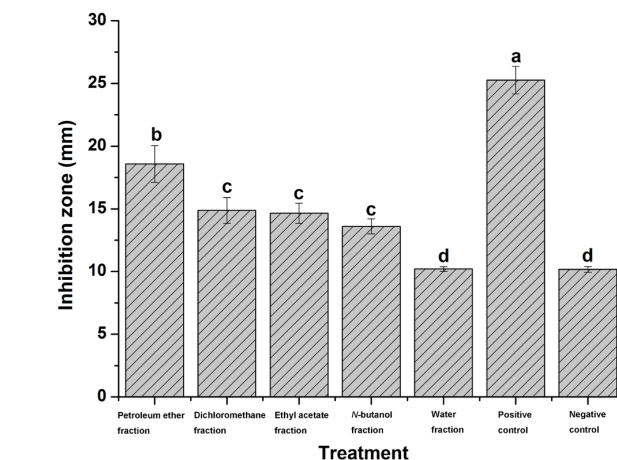


Fig. 1: Antimicrobial activity of five fractions from *Athyrium sinense* against *Clavibacter michiganensis* subsp. *sepedonicus* (Cms). Different letters indicated significant difference ($P < 0.05$), and each inhibitory test was performed three times. DMSO dissolved in distilled water to a concentration of 20% (v/v) was used as the control. The diameter of hole was 10 mm, and 20% DMSO had no notable antimicrobial activity against *Clavibacter michiganensis* subsp. *sepedonicus* (Cms). The data were expressed as mean \pm standard deviation of three technical replicates (three inhibition tests using the same extract).

acid (0.79%), dihydroactinidiolide (0.48%), monomethyl succinate (0.48%), 2-methyl-2-pentenoic acid (0.41%), 17-octadecynoic acid (0.36%), 4,8,12,16-tetramethylheptadecan-4-olide (0.36%), and butyl 3-hydroxybutyrate (0.32%).

Tab. 1: Constituents of petroleum ether fraction (PA) from *Athyrium sinense*.

No.	RT(min) ^a	RI ^b	Compounds	Molecular formula	Peak area (%)
1	4.11	956.90	3-Methylvaleric acid	C ₆ H ₁₂ O ₂	2.21
2	4.31	969.00	2-Methyl-2-pentenoic acid	C ₆ H ₁₀ O ₂	0.41
3	6.24	1084.10	Butyl 3-Hydroxybutyrate	C ₈ H ₁₆ O ₃	0.32
4	7.58	1142.90	Monomethyl succinate	C ₅ H ₈ O ₄	0.48
5	10.41	1248.50	Phenylacetic acid	C ₈ H ₈ O ₂	1.01
6	10.99	1268.60	Nonanoic acid	C ₉ H ₁₈ O ₂	1.04
7	16.04	1440.10	2-Hydroxy-5-methylbenzaldehyde	C ₈ H ₈ O ₂	1.15
8	18.75	1532.80	Dihydroactinidiolide	C ₁₁ H ₁₆ O ₂	0.48
9	21.85	1642.70	Phloretic acid	C ₉ H ₁₀ O ₃	7.48
10	25.05	1761.00	Myristic acid	C ₁₄ H ₂₈ O ₂	0.79
11	27.09	1839.60	Neophytadiene	C ₂₀ H ₃₈	13.66
12	27.71	1864.10	<i>E</i> -11-Hexadecen-1-ol	C ₁₆ H ₃₂ O	6.10
13	28.16	1881.80	1-Hexadecanol	C ₁₆ H ₃₄ O	5.41
14	30.28	1970.20	Palmitic acid	C ₁₆ H ₃₂ O ₂	25.78
15	30.88	1995.80	Palmitic acid ethyl ester	C ₁₈ H ₃₆ O ₂	0.93
16	32.10	2047.20	—	—	2.30
17	33.12	2090.40	Methyl sinapate	C ₁₂ H ₁₄ O ₅	6.92
18	33.63	2113.10	3,7,11,15-Tetramethyl-2-hexadecen-1-ol	C ₂₀ H ₄₀ O	1.10
19	34.14	2135.90	Linoleic acid	C ₁₈ H ₃₂ O ₂	8.95
20	34.27	2141.70	Oleic acid	C ₁₈ H ₃₄ O ₂	8.20
21	34.75	2163.20	Stearic acid	C ₁₈ H ₃₆ O ₂	2.87
22	35.97	2220.30	17-Octadecynoic acid	C ₁₈ H ₃₂ O ₂	0.36
23	38.78	2363.00	4,8,12,16-Tetramethylheptadecan-4-olide	C ₂₁ H ₄₀ O ₂	0.36
24	40.13	2431.70	—	—	0.82
25	41.67	2510.00	Pentacosane	C ₂₅ H ₅₂	0.87

^a RT=Retention time.

^b RI=Calculated retention index.

“—” meant that the component was not identified.

Electron microscopy

In electronic micrographs, the control Cms cells showed normal morphologies with smooth surfaces, regular shapes, and dense cytoplasm adhered to cell membrane and cell wall (Fig. 2 a and d). Compared with control, Cms cells treated with 0.20 mg mL⁻¹ of PA underwent morphological alterations (Fig. 2 b, c, e and f). The damaged Cms cells were adhered together (Fig. 2; 1, 2) and seriously collapsed (Fig. 2; 3 and 4). Some Cms cells were misshapen and disproportionate (Fig. 2; 5, 7, 8 and 9). Some Cms cells exhibited large vacuoles (Fig. 2; 5, 6, 7, 9 and 10).

Characterizations of cell wall and cell membrane

Fig. 3 showed the antimicrobial effect of PA on the integrity of cell wall and the permeability of cell membrane. When concentrations of PA were 0.10 mg mL⁻¹, 0.15 mg mL⁻¹, and 0.20 mg mL⁻¹, the AKP activities in supernatant were significantly increased ($P < 0.05$) as compared to control (Fig. 3 a). In extracellular soluble protein assay, when concentrations of PA were 0.05 mg mL⁻¹ and 0.10 mg mL⁻¹, there was no significant difference between control and treatment (Fig. 3 b). When the concentration was greater than 0.10 mg mL⁻¹, the extracellular soluble protein increased ($P < 0.05$) significantly (Fig. 3 b).

Characterizations of intracellular materials

As shown in Fig. 4, when concentrations of PA were 0.05 mg mL⁻¹, 0.10 mg mL⁻¹, 0.15 mg mL⁻¹ and 0.20 mg mL⁻¹, the ATPase activities were decreased significantly ($P < 0.05$; Fig. 4 a). In DNA content assay, when concentration of PA was 0.05 mg mL⁻¹, there was no significant difference between control and treatment (Fig. 4 b). When the concentration was greater than 0.05 mg mL⁻¹, DNA fluorescence intensities decreased ($P < 0.05$) significantly (Fig. 4 b).

Determination of membrane potential

In Fig. 5, the fluorescence intensity of membrane potential in control was 254.80. When concentrations of PA were 0.05 mg mL⁻¹, 0.10 mg mL⁻¹ and 0.15 mg mL⁻¹, the fluorescence intensity of membrane potential decreased to 118.62, 79.44 and 74.81, respectively.

Determination of cell cycle

There are three stages in bacterial cell cycle, I phase (equivalent to G1 phase in Fig. 6), R phase (equivalent to S phase in Fig. 6), and D phase. When R phase was completed, the prokaryote directly entered into D phase without G2 phase (Li et al., 2015). As shown in Fig. 6, I phase of Cms cells increased to 35.93% (0.05 mg mL⁻¹ of PA), 37.20% (0.10 mg mL⁻¹ of PA), and 43.90% (0.15 mg mL⁻¹ of PA), compared to the value of 34.74% in control cells. The R phase of Cms cells decreased to 63.57% (0.05 mg mL⁻¹ of PA), 62.80% (0.10 mg mL⁻¹ of PA), and 56.10% (0.15 mg mL⁻¹ of PA), compared to the value of 65.26% in control cells.

Discussion

Cms causes bacterial ring rot in potato growing areas, which is difficult to control and can cause serious economic losses (STEVENS et al., 2017). However, there are a few reports of plant extracts, which have antimicrobial activity against Cms. WU (2014) had reported that *Artemisia annua*, *Artemisia argyi*, *Artemisia capillaries*, *Artemisia sieversiana*, *Artemisia mongolica*, *Artemisia sylvatica* had antimicrobial activities against Cms and the inhibitory zone was ranged from 9 mm to 10.7 mm. In this study, PA had an obvious inhibitory effect on Cms (Fig. 1). The inhibitory zone of PA was 18.58 mm, which was higher than that of WU reported in the literature (WU, 2014).

GC-MS analysis (Tab. 1) identified twenty-five components in PA. Organic acids occupied the main component of 59.10%. HSIAO and

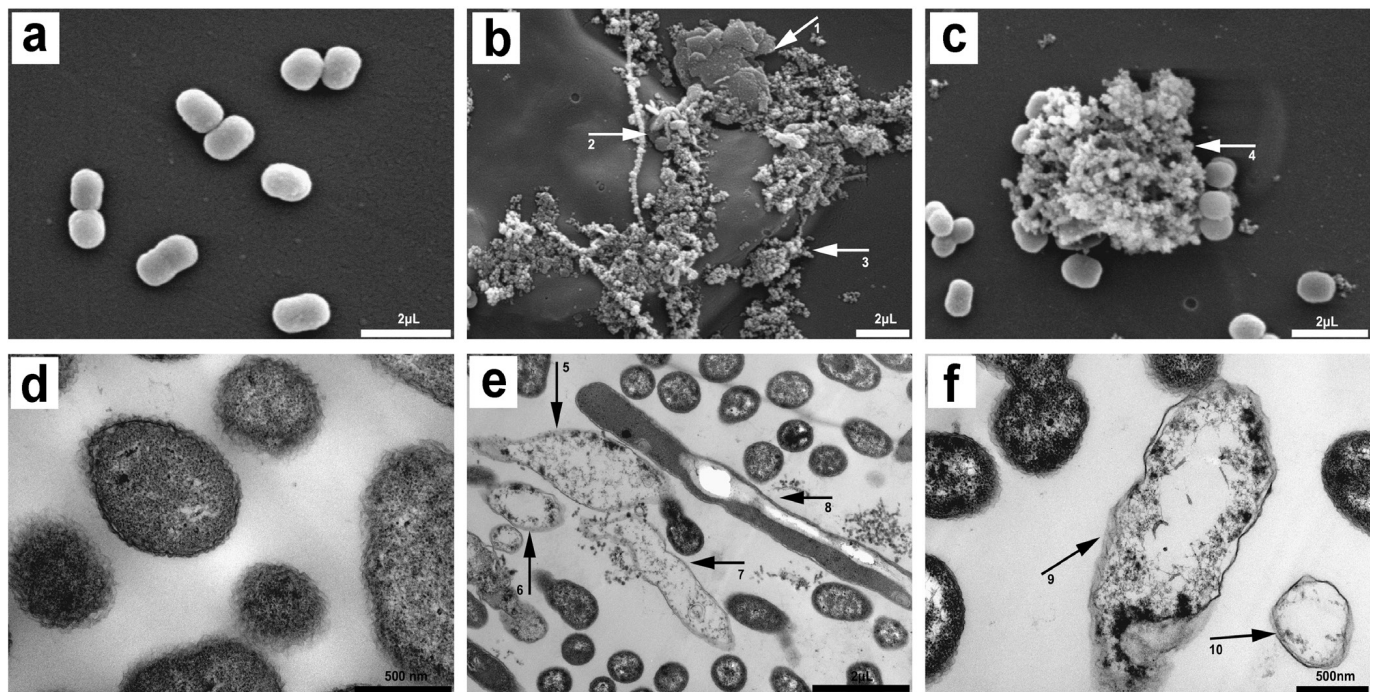


Fig. 2: Scanning electron microscope (SEM) and transmission electron microscope (TEM) photographs of *Clavibacter michiganensis* subsp. *sepedonicus* (Cms). Control (a 10000x and d 80000x), Cms cells treated with 0.80% DMSO. Treatment (b 6000x, c 8600x, e 20000x, and f 60000x), Cms cells treated with bioassay-guided fraction from *A. sinense* (PA) at the concentration of 0.20 mg/mL. Cms cells were adhered together (1 and 2), were seriously collapsed (3 and 4), showed anomalous shapes (5, 7, 8 and 9), and exhibited large vacuoles (5, 6, 7, 9 and 10).

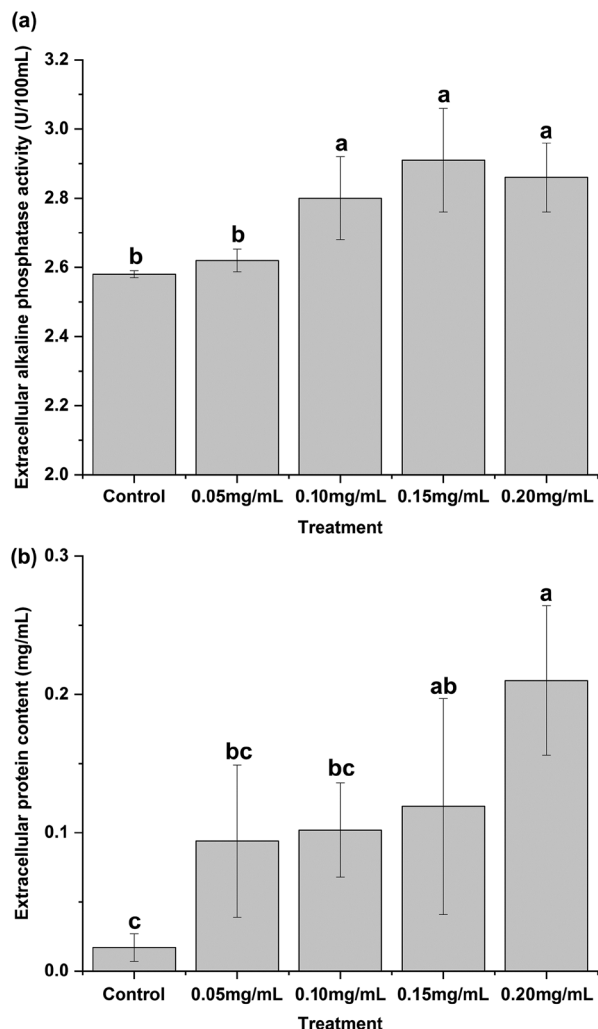


Fig. 3: Release of alkaline phosphatase (AKP; a) and release of soluble protein (b). Control was *Clavibacter michiganensis* subsp. *sepedonicus* (Cms) cells treated with 0.80% DMSO. Data were expressed as the mean \pm standard deviation of three technical replicates (three tests using the same extract). Different letters represented significant differences ($P < 0.05$).

SIEBERT (1999) reported that organic acids played an important role in inhibiting bacteria through interacting with phospholipid molecules and lipopolysaccharides in cell membrane (HSIAO and SIEBERT, 1999). Organic acids caused the appearance of protonated phosphate groups, which could decrease the interaction among different components in the outer membrane, and further lead to the leakage of intracellular contents (ALAKOMI et al., 2000). Palmitic acid (25.78%), linoleic acid (8.95%), oleic acid (8.20%), and stearic acid (2.87%) were the predominant components of organic acids in PA. These organic acids were also determined as the main compounds of other plant extracts, which showed antifungal activity. SILVA et al. (2018) reported the *n*-hexane fraction of *Osmundea pinnatifida* (Rhodophyta) had a remarkable antifungal activity, and it contained 29.60% of palmitic acid, 9.60% of oleic acid and 6.20% of stearic acid. *Gailonia aucheri* oil showed antimicrobial activity against *E. coli*, *S. epidermis* and *A. niger*, and the major components of *G. aucheri* oil were myristicin (32.80%) and oleic acid (9.20%) (ZEKAVATI et al., 2018). *Momordica charantia* exhibited obvious activities for inhibiting *Salmonella typhi* and *Klebsiella pneumoniae*, and 37.60% of *M. charantia* was stearic acid (ZUBAIR et al., 2018). *Nigella sativa*

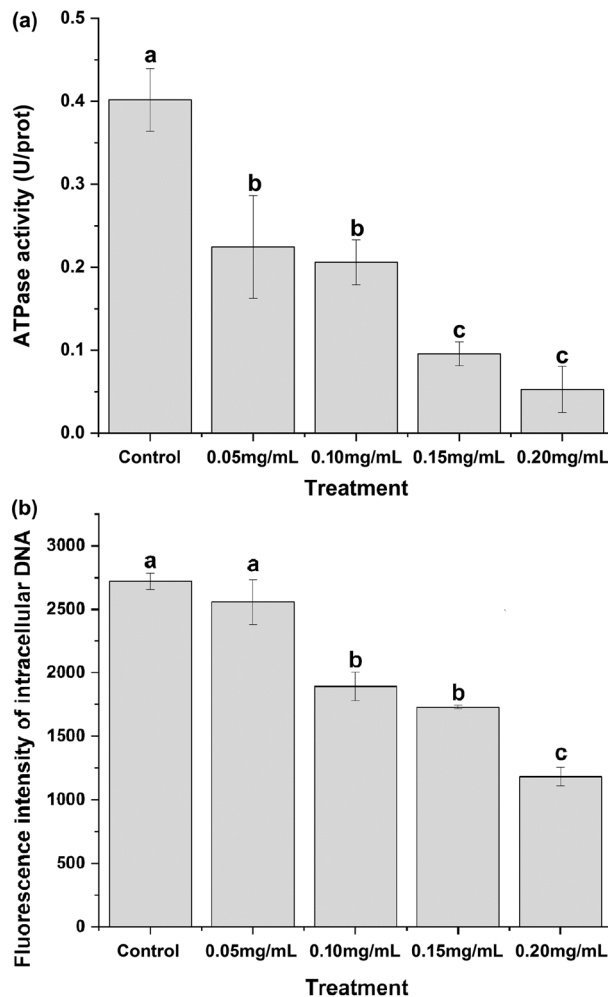


Fig. 4: Effects of bioassay-guided fraction from *Athyrium sinense* (PA) on intracellular ATPase activity and DNA content in *Clavibacter michiganensis* subsp. *sepedonicus* (Cms). Control was Cms cells treated with 0.80% DMSO. Data were expressed as the mean of three technical replicates (three tests using the same extract) \pm standard deviation. Different letters represented significant differences ($P < 0.05$).

oil was demonstrated to have antimicrobial activity against food-borne bacteria, and linoleic acid was the main compound (MOUWAKEH et al., 2018). In addition, neophytadiene (PALIC et al., 2002), nonanoic acid (WANG et al., 2013), palmitic acid ethyl ester (YAO et al., 2013), pentacosane (WEI and PENG, 2016), and myristic acid (ALTIERI et al., 2009) had been reported as antimicrobial compounds or as the main compounds in antimicrobial plant extracts. Therefore, PA might take effects on Cms inhibition through the cooperation of these active compounds.

SEM and TEM were performed to observe the microstructure changes of Cms. After exposure to PA, Cms cells presented distinctive damages including the formation of adhesive cells, appearance of large vacuoles, leakage of intracellular protoplasm, and cell lysis (Fig. 2). The results indicated these active compounds of PA might penetrate through cell membrane, causing the leakage of intracellular substances (XU et al., 2018). Subsequently, the damaged cell membrane led to vacuole formations and Cms death. These findings confirmed the strong antimicrobial activity of PA, and also indicated that cell membrane of Cms might be the main target.

Cell walls and cell membranes are the critical structural components

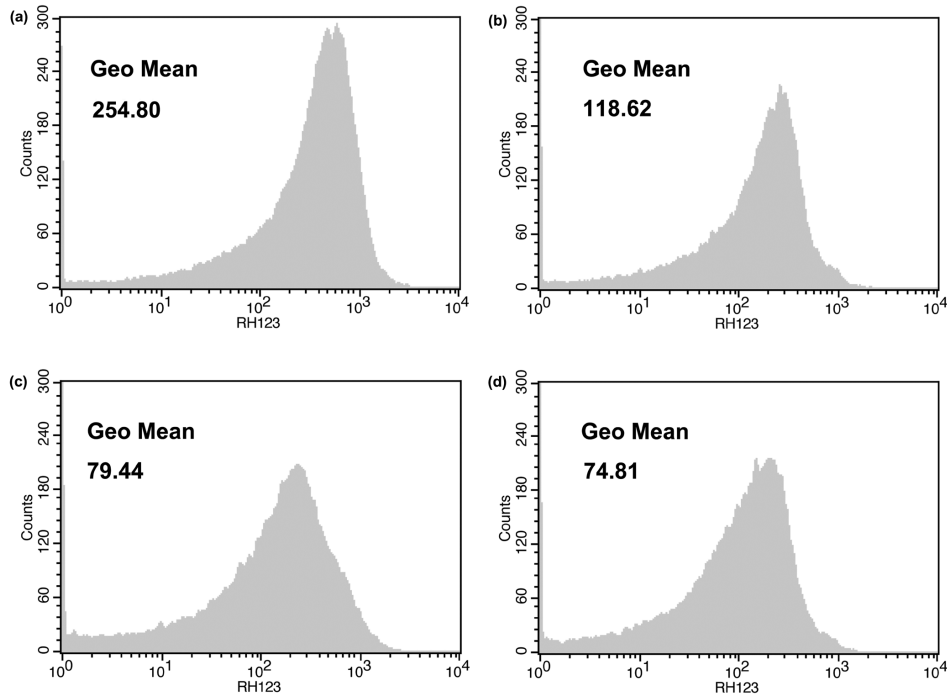


Fig. 5: Effect of bioassay-guided fraction from *Athyrium sinense* (PA) on membrane potential of *Clavibacter michiganensis* subsp. *sepedonicus* (Cms). Cms cells were treated with 0.80% DMSO (control, a); Cms cells were treated with PA at the concentration of 0.05 mg mL⁻¹ (b); Cms cells were treated with PA at the concentration of 0.10 mg mL⁻¹ (c); and Cms cells were treated with PA at the concentration of 0.15 mg mL⁻¹ (d).

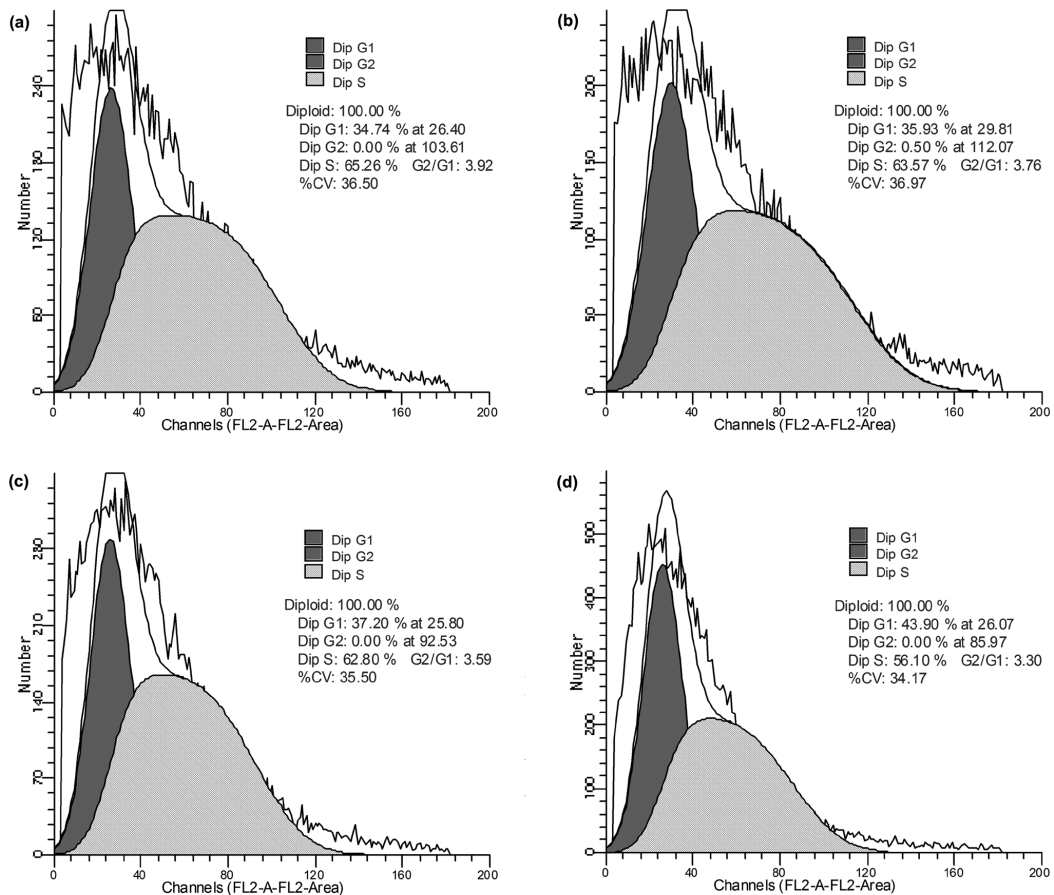


Fig. 6: Effect of bioassay-guided fraction from *Athyrium sinense* (PA) on cell cycle of *Clavibacter michiganensis* subsp. *sepedonicus* (Cms). Cms cells were treated with 0.80% DMSO (control, a); Cms cells were treated with PA at the concentration of 0.05 mg mL⁻¹ (b); Cms cells were treated with PA at the concentration of 0.10 mg mL⁻¹ (c); Cms cells were treated with PA at the concentration of 0.15 mg mL⁻¹ (d).

of bacteria. AKP is mainly located between bacterial cell wall and bacterial cell membrane (MA et al., 2013). It will be leaked, when cell walls are damaged (HE et al., 2018). Therefore, extracellular AKP activity reflects the integrity of cell wall. As shown in Fig. 3, extracellular AKP activity increased significantly, when concentration of PA was 0.10 mg mL⁻¹, 0.15 mg mL⁻¹, and 0.20 mg mL⁻¹. The results showed a positive correlation between AKP leakage and PA concentration. When bacterial cell membranes are damaged, intracellular soluble protein can be detected outside the cells. Fig. 3 showed that the extracellular soluble protein increased significantly, when concentration of PA increased to 0.15 mg mL⁻¹ and 0.20 mg mL⁻¹. It was indicated that PA had a detrimental effect on cell membrane integrity, causing the leakage of intracellular soluble protein.

ATPase plays an important role in transporting active substance across cell membrane. It was used to assess available energy states in a microorganism and to reflect the cell metabolic status (FEI et al., 2018). After treatment with PA, the intracellular ATPase activity decreased ($P < 0.05$) significantly as compared to control (Fig. 4). The result revealed that ATPase activity was inhibited by PA. Moreover, the reduction of ATPase activity might be due to the excessive membrane permeability, and might lead to the hydrolysis of intracellular ATP. DNA controls bacterial growth, protein synthesis, and bacterial metabolism (CUI et al., 2018). Fig. 4 showed that the intracellular DNA contents decreased significantly, when concentration of PA was greater than 0.05 mg/mL. It seems that when cell membrane of *Cms* was destroyed, small molecules should release from *Cms* cells firstly, followed by macromolecules, such as DNA. It implied that PA might inhibit the nucleic acid synthesis, leading to a drastic decrease in DNA content.

Membrane potential is an essential parameter of bacteria. The depolarization of cell membrane can lead to irregular metabolic activity and cell membrane disruption (KANG et al., 2018). In Fig. 5, when *Cms* cells were treated by PA, cell membrane potential decreased remarkably as compared to control group. The result indicated that the depolarization of cell membrane occurred rapidly, when *Cms* cells were exposed to PA. More importantly, the active compounds in PA might easily insert into the depolarized cell membrane, resulting in cell death ultimately.

In bacterial cell cycle, the preparation phase of DNA replication is represented by I and DNA replicating phase is represented by R (LI et al., 2015). Fig. 6 exhibited an increasing value of I phase (35.93%, 37.20%, and 43.90% respectively) and a decreasing value of R phase (63.57%, 62.80%, and 56.10% respectively). The result indicated that PA penetrated through the damaged cell membrane and attached the nucleic acid, leading to most *Cms* cells to remain in I phase.

Conclusion

We demonstrated that PA was a fraction with a strong antimicrobial activity against *Cms*. GC-MS analysis revealed that the main components of PA were palmitic acid (25.78%), linoleic acid (8.95%), oleic acid (8.20%), and phloretic acid (7.48%). Based on the results of SEM, TEM, extracellular AKP activity, extracellular soluble protein, ATPase activity, DNA content assay, membrane potential, and cell cycle, we concluded that cell membrane of *Cms* should be the main target, which was destroyed by PA. We expect that PA could be used as an alternative bactericide for controlling *Cms* growth.

Acknowledgments

This study was supported by National Natural Science Foundation of China (No.31601677), Natural Science Foundation of Shanxi Province, China (No.201701D221179), and Scientific and Technological Innovation Programs of Higher Education Institutions in Shanxi Province, China (STIP; No.2016117).

Conflict of interest

No potential conflict of interest was reported by the authors.

References

- ALAKOMI, H.L., SKYTÄ, E., SAARELA, M., MATTILA-SANDHOLM, T., LATVA-KALA, K., HELANDER, I.M., 2000: Lactic acid permeabilizes gram-negative bacteria by disrupting the outer membrane. *Appl. Environ. Microb.* 66, 2001-2005. DOI: [10.1128/AEM.66.5.2001-2005.2000](https://doi.org/10.1128/AEM.66.5.2001-2005.2000)
- ALTIERI, C., BEVILACQUA, A., CARDILLO, D., SINIGAGLIA, M., 2009: Antifungal activity of fatty acids and their monoglycerides against *Fusarium* spp. in a laboratory medium. *Int. J. Food Sci. Tech.* 44, 242-245. DOI: [10.1111/j.1365-2621.2007.01639.x](https://doi.org/10.1111/j.1365-2621.2007.01639.x)
- ASANO, T., MIWA, A., MAEDA, K., KIMURA, M., NISHIUCHI, T., 2013: The secreted antifungal protein thionin 2.4 in *Arabidopsis thaliana* suppresses the toxicity of a fungal fruit body lectin from *Fusarium graminearum*. *Plos Pathog.* 9, e1003581. DOI: [10.1371/journal.ppat.1003581](https://doi.org/10.1371/journal.ppat.1003581)
- BEHBAHANI, B.A., SHAHIDI, F., YAZDI, F.T., MORTAZAVI, S.A., MOHEBBI, M., 2017: Antioxidant activity and antimicrobial effect of tarragon (*Artemisia dracunculus*) extract and chemical composition of its essential oil. *J. Food Meas. Charact.* 11, 847-863. DOI: [10.1007/s11694-016-9456-3](https://doi.org/10.1007/s11694-016-9456-3)
- CAI, J., FENG, J., WANG, F., XU, Q., XIE, S., 2014: Antibacterial activity of petroleum ether fraction from *Laminaria japonica* extracts against *Clavibacter michiganensis* subsp. *sepedonicus*. *Eur. J. Plant Pathol.* 140, 291-300. DOI: [10.1007/s10658-014-0462-1](https://doi.org/10.1007/s10658-014-0462-1)
- CAI, J., FENG, J., XIE, S., 2015: Inhibitory activity of *Athyrium sinense* extracts against *Clavibacter michiganensis* subsp. *sepedonicum*. *J. Appl. Bot. Food Qual.* 88, 314-321. DOI: [10.5073/JABFQ.2015.088.045](https://doi.org/10.5073/JABFQ.2015.088.045)
- CHO, M.S., PARK, D.H., NAMGUNG, M., AHN, T.Y., PARK, D.S., 2015: Validation and application of a real-time PCR protocol for the specific detection and quantification of *Clavibacter michiganensis* subsp. *sepedonicus* in potato. *Plant Pathology J.* 31, 123-131. DOI: [10.5423/PPJ.OA.02.2015.0019](https://doi.org/10.5423/PPJ.OA.02.2015.0019)
- CONG, H.Y., ZHAO, H., 2010: Study on medicinal pteridophytes resources in Kunyu Mountain in Shandong province. *Lishizhen Med. Materia Medica Res.* 21, 3276-3278. DOI: [10.1360/972010-1292](https://doi.org/10.1360/972010-1292)
- CUI, H.Y., ZHANG, C.H., LI, C.Z., LIN, L., 2018: Antimicrobial mechanism of clove oil on *Listeria monocytogenes*. *Food Control* 94, 140-146. DOI: [10.1016/j.foodcont.2018.07.007](https://doi.org/10.1016/j.foodcont.2018.07.007)
- ELOFF, J.N., ANGEH, I.E., MCGAW, L.J., 2017: Solvent-solvent fractionation can increase the antifungal activity of a *Melianthus comosus* (Melianthaceae) acetone leaf extract to yield a potentially useful commercial antifungal product. *Ind. Crop. Prod.* 110, 103-112. DOI: [10.1016/j.indcrop.2017.11.014](https://doi.org/10.1016/j.indcrop.2017.11.014)
- ENDO, E.H., CORTEZ, D.A., UEDA-NAKAMURA, T., NAKAMURA, C.V., DIAS FILHO, B.P., 2010: Potent antifungal activity of extracts and pure compound isolated from pomegranate peels and synergism with fluconazole against *Candida albicans*. *Res. Microbiol.* 161, 534-540. DOI: [10.1016/j.resmic.2010.05.002](https://doi.org/10.1016/j.resmic.2010.05.002)
- FEI, P., ALI, M.A., GONG, S.Y., SUN, Q., BI, X., LIU, S.F., GUO, L., 2018: Antimicrobial activity and mechanism of action of olive oil polyphenols extract against *Cronobacter sakazakii*. *Food Control* 94, 289-294. DOI: [10.1016/j.foodcont.2018.07.022](https://doi.org/10.1016/j.foodcont.2018.07.022)
- HE, N., WANG, P.Q., WANG, P.Y., MA, C.Y., KANG, W.Y., 2018: Antibacterial mechanism of chelerythrine isolated from root of *Toddalia asiatica* (Linn) Lam. *BMC Complem. Altern. M.* 18, 261. DOI: [10.1186/s12906-018-2317-3](https://doi.org/10.1186/s12906-018-2317-3)
- HOLTSMARK, I., TAKLE, G.W., BRURBERG, M.B., 2008: Expression of putative virulence factors in the potato pathogen *Clavibacter michiganensis* subsp. *sepedonicus* during infection. *Arch. Microbiol.* 189, 131-139. DOI: [10.1007/s00203-007-0301-2](https://doi.org/10.1007/s00203-007-0301-2)
- HSHAO, C.P., SIEBERT, K.J., 1999: Modeling the inhibitory effects of organic acids on bacteria. *Int. J. Food Microbiol.* 47, 189-201. DOI: [10.1016/S0168-1605\(99\)00012-4](https://doi.org/10.1016/S0168-1605(99)00012-4)

- KANG, J., LIU, L., WU, X., SUN, Y., LIU, Z., 2018: Effect of thyme essential oil against *Bacillus cereus* planktonic growth and biofilm formation. *Appl. Microbiol. Biot.* 102, 10209-10218. DOI: [10.1007/s00253-018-9401-y](https://doi.org/10.1007/s00253-018-9401-y)
- LI, L.R., SHI, Y.H., CHENG, X.R., XIA, S.F., CHESEREK, M.J., LE, G.W., 2015: A cell-penetrating peptide analogue, P7, exerts antimicrobial activity against *Escherichia coli* ATCC25922 via penetrating cell membrane and targeting intracellular DNA. *Food Chem.* 166, 231-239. DOI: [10.1016/j.foodchem.2014.05.113](https://doi.org/10.1016/j.foodchem.2014.05.113)
- MA, Y., LIU, Z., YANG, Z., LI, M., LIU, J., SONG, J., 2013: Effects of dietary live yeast *Hanseniaspora opuntiae* C21 on the immune and disease resistance against *Vibrio splendidus* infection in juvenile sea cucumber *Apostichopus japonicus*. *Fish Shellfish Immun.* 34, 66-73. DOI: [10.1016/j.fsi.2012.10.005](https://doi.org/10.1016/j.fsi.2012.10.005)
- MDEE, L.K., MASOKO, P., ELOFF, J.N., 2009: The activity of extracts of seven common invasive plant species on fungal phytopathogens. *S. Afr. J. Bot.* 75, 375-379. DOI: [10.1016/j.sajb.2009.02.003](https://doi.org/10.1016/j.sajb.2009.02.003)
- MONSÁLVEZ, M., ZAPATA, N., VARGAS, M., BERTI, M., BITTNER, M., HERNÁNDEZ, V., 2010: Antifungal effects of n-hexane extract and essential oil of *Drimys winteri* bark against Take-All disease. *Ind. Crop. Prod.* 31, 239-244. DOI: [10.1016/j.indcrop.2009.10.013](https://doi.org/10.1016/j.indcrop.2009.10.013)
- MOUWAKEH, A., RADACSI, P., PLUHAR, Z., ZAMBORINE, E.N., MURANSZKY, G., MOHACSI-FARKAS, C., KISKO, G., 2018: Chemical composition and antimicrobial activity of *Nigella sativa* crude and essential oil. *Acta Aliment. Hung.* 47, 379-386. DOI: [10.1556/066.2018.47.3.14](https://doi.org/10.1556/066.2018.47.3.14)
- NISSINEN, R., KASSUWI, S., PELTOLA, R., METZLER, M.C., 2001: In planta-complementation of *Clavibacter michiganensis* subsp. *sepedonicus* strains deficient in cellulose production or HR induction restores virulence. *Eur. J. Plant Pathol.* 107, 175-182. DOI: [10.5197/j.2044-0588.2016.033.007](https://doi.org/10.5197/j.2044-0588.2016.033.007)
- PALIC, R., STOJANOVIĆ, G., ALAGIC, S.Č., NIKOLIC, M., LEPOJEVIC Z., 2002: Chemical composition and antimicrobial activity of the essential oil and CO₂ extracts of the oriental tobacco, *Prilep*. *Flavour Frag. J.* 17, 323-326. DOI: [10.1002/ffj.1084](https://doi.org/10.1002/ffj.1084)
- PIRAS, A., GONÇALVES, M.J., ALVES, J., FALCONIERI, D., PORCEDDA, S., MAXIA, A., SALGUEIRO, L., 2018: *Ocimum tenuiflorum* L. and *Ocimum basilicum* L., two spices of Lamiaceae family with bioactive essential oils. *Ind. Crop. Prod.* 113, 89-97. DOI: [10.1016/j.indcrop.2018.01.024](https://doi.org/10.1016/j.indcrop.2018.01.024)
- SILVA, P.J., FERNANDES, C., BARROS, L., FERREIRA, I.C.F.R., PEREIRA, L. GONÇALVES, T., 2018: The antifungal activity of extracts of *Osmunda pinnatifida*, an edible seaweed, indicates its usage as a safe environmental fungicide or as a food additive preventing post-harvest fungal food contamination. *Food Funct.* 9, 6188-6196. DOI: [10.1039/C8FO01797B](https://doi.org/10.1039/C8FO01797B)
- STEVENS, L.H., LAMERS, J.G., VAN DER ZOUWEN, P.S., MENDES, O., VAN DEN BERG, W., TJOU-TAM-SIN, N.N.A., JILESEN, C.J.T.J., SPOORENBERG, P.M. VAN DER WOLF, J.M., 2017: Chemical eradication of the ring rot bacterium *Clavibacter michiganensis* subsp. *sepedonicus* on potato storage crates. *Potato Res.* 60, 145-158. DOI: [10.1007/s11540-017-9342-3](https://doi.org/10.1007/s11540-017-9342-3)
- WANG, C.Q., PAN, S.J., ZUO, G.F., WANG, Z.B., LUO, Y., 2013: GC-MS analysis of chemical composition and antibacterial activity of volatile oil from flowers of *Elaeagnus lanceolata* Warb. *apud Diels. Food Sci.* 34, 191-193.
- WEI, Q., PENG, X.Y., 2016: Chemical components of essential oils of the flower, leaf-stem and fruit from *Amygdalus persica* var. *persica* f. *duplex* and their antioxidant, antimicrobial effects. *Chinese J. Appl. Chem.* 33, 945-950.
- WU, Y.H., 2014: Comparative study on antibacterial effect about plant extracts of six species of *Artemisia* L. plants. *North. Hortic.* 2014, 121-125.
- XIANG, F., BAI, J.H., TAN, X.B., CHEN, T., YANG, W., HE, F., 2018: Antimicrobial activities and mechanism of the essential oil from *Artemisia argyi* Levl. et Van. var. *argyi* cv. Qiai. *Ind. Crop. Prod.* 125, 582-587. DOI: [10.1016/j.indcrop.2018.09.048](https://doi.org/10.1016/j.indcrop.2018.09.048)
- XU, L.C., TAO, N.G., YANG, W.H., JING, G.X., 2018: Cinnamaldehyde damaged the cell membrane of *Alternaria alternata* and induced the degradation of mycotoxins *in vivo*. *Ind. Crop. Prod.* 112, 427-433. DOI: [10.1016/j.indcrop.2017.12.038](https://doi.org/10.1016/j.indcrop.2017.12.038)
- YANG, M.H., YANG, X.Q., WANG, G.S., DING, Z.T., 2008: Advances in chemical constituents and pharmacological activities of *Athyrium* in China. *China Pharm.* 18, 1189-1191.
- YAO, X., YUE, Y.D., TANG, F., 2013: GC/MS analysis of volatile oil of culm and leaves from *D. farinosus* and evaluation of its inhibiting ability to bacteria. *Chinese J. Spectrosc. Lab.* 30, 2344-2350.
- YUAN, W.Q., YUK, H.G., 2018: Antimicrobial efficacy of *Syzygium anti-septicum* plant extract against *Staphylococcus aureus* and methicillin-resistant *S. aureus* and its application potential with cooked chicken. *Food Microbiol.* 72, 176-184. DOI: [10.1016/j.fm.2017.12.002](https://doi.org/10.1016/j.fm.2017.12.002)
- ZEKAVATI, R., FARJAM, M.H., DOULAH, A., 2018: Chemical compositions of essential oil of *Gailonia aucheri* from Iran and its antimicrobial and antioxidant activities and total phenol content. *Iranlan J. Sci. Technol. T.* 42, 1125-1130. DOI: [10.1007/s40995-017-0168-2](https://doi.org/10.1007/s40995-017-0168-2)
- ZHONG, F.L., WANG, W.J., WANG, X.L. LUO, Y.H., 2016: Research on the antioxidant ability of total flavonoids in *Athyrium multidentatum* and *Polygonatum odoratum* (Mill.) *Druce* *in vitro*. *China Food Addit.* 6, 65-72.
- ZUBAIR, M.F., ATOLANI, O., IBRAHIM, S.O., OGUNTOYE, O.S., ABDULRAHIM, H.A., OYEGOKE, R.A., OLATUNJI, G.A., 2018: Chemical and biological evaluations of potent antiseptic cosmetic products obtained from *Momordica charantia* seed oil. *Sust. Chem. Pharm.* 9, 35-41. DOI: [10.1016/j.scp.2018.05.005](https://doi.org/10.1016/j.scp.2018.05.005)

ORCID


Jin Cai  <https://orcid.org/0000-0003-1597-8143>Beibei Du  <https://orcid.org/0000-0002-2386-8975>

Address of the corresponding author:

Jin Cai, Institute of Applied Chemistry, Shanxi University, Taiyuan 030006, China

E-mail: caijin@sxu.edu.cn

© The Author(s) 2020.

 This is an Open Access article distributed under the terms of the Creative Commons Attribution 4.0 International License (<https://creativecommons.org/licenses/by/4.0/deed.en>).